Scintillation properties of some Ce^{3+} and Pr^{3+} doped inorganic crystals*

P. Dorenbos, R. Visser, C.W.E. van Eijk,
Radiation Technology Group, Department of Applied Physics,
Delft University of Technology, Mekelweg 15, 2629 JB Delft, the Netherlands

N.M. Khaidukov
N.S. Kurnakov Institute of General and Inorganic Chemistry, Moscow, Russia

M.V. Korzhik
Institute of Nuclear Problems, Minsk, Belorussia

Abstract

The scintillation properties of Ce^{3+} and Pr^{3+} doped complex fluoride crystals of composition $CsGd_2F_7$ and K_2YF_5 and of Pr^{3+} doped $Y_3Al_5O_{12}$ single crystals were studied by means of x-ray and gamma ray excitation. The Ce^{3+} and Pr^{3+} doped fluoride crystals show 5d-4f luminescences at wavelengths near 340 nm and 240 nm, respectively. 5d-4f luminescence of Pr^{3+} doped $Y_3Al_5O_{12}$ is observed between 300 and 400 nm. We present the absolute light yield in photons/MeV together with results from scintillation decay time experiments.

Introduction

In the search for new fast scintillators with a luminescence decay time of ≤ 20 ns, two types of luminescence are of importance. i) *5d-4f luminescence* caused by electron transitions in rare earth impurities. These transitions are allowed according to the electric dipole approximation, and consequently the radiative decay is relatively fast. Fast 5d-4f transitions were observed for crystals doped with Ce^{3+}, Pr^{3+}, and Nd^{3+}. Especially Ce^{3+} has been studied as an activator in scintillation crystals [1, 2, 3, 4, 5, 6]. Nd^{3+} doped in suitable host crystals shows 5d-4f luminescence at vacuum ultra-violet wavelengths, i.e. at wavelengths shorter than 190 nm [7]. The scintillation properties of Pr^{3+} doped host crystals have not been studied much yet. ii) *cross-luminescence*. This intrinsic luminescence mechanism can be observed in ionic crystals in which the energy gap between the conduction band and the anion valence band is larger than the energy between the top of the anion valence band and the top of the uppermost cation core band [8, 9]. This situation can be expected for compounds containing K^+, Rb^+, Cs^+, or Ba^{2+} cations together with F^- anions. Some Rb^+ and Cs^+ based chloride compounds are also known for their cross-luminescence properties.

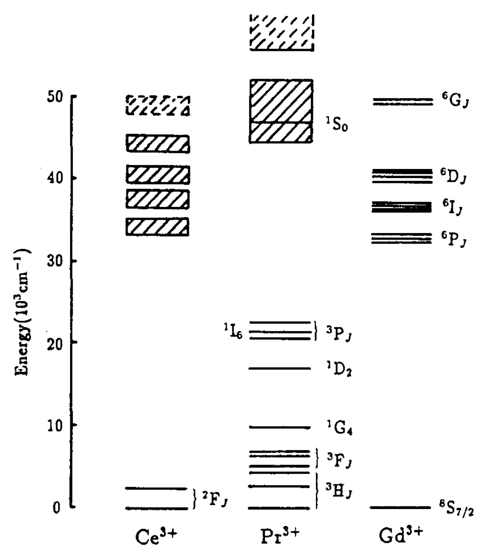

Figure 1: 4f and 5d energy level diagrams of Ce^{3+} in $CsGd_2F_7$, Pr^{3+} in K_2YF_5, and Gd^{3+}.

In this work we studied the scintillation properties of Ce^{3+} and Pr^{3+} doped $CsGd_2F_7$, Pr^{3+} doped K_2YF_5, and Pr^{3+} doped $Y_3Al_5O_{12}$ crystals. Figure 1 shows the energy level diagrams of the trivalent rare earth ions Ce^{3+}, Pr^{3+}, and Gd^{3+} with ground state electron configurations $4f^1$, $4f^2$, and $4f^7$ respectively. The narrow energy levels belong to states of the $4f^n$ configurations. The positions of these states are almost independent of the type of host crystal [10]. The shaded regions in Figure 1 show the positions of the 5d bands as determined from optical absorption experiments. The location and the number of excited 5d bands depend strongly on the interaction of the 5d electron with the host crystal. A crystal field with a low point symmetry

*These investigations in the program of the Foundation for Fundamental Research on Matter (FOM) have been supported by the Netherlands Technology Foundation (STW)

0018-9499/93$03.00 © 1993 IEEE

at a rare earth site will split the degenerate 5d levels into 5 distinct sublevels. This is probably the case for Ce^{3+} ions doped in $CsGd_2F_7$. The four lowest energy 4f-5d absorption bands were observed in the optical absorption spectra at 290, 265, 245, and 225 nm. The fifth band is assumed to be located near 203 nm. Pr^{3+} doped K_2YF_5 shows a broad 4f-5d absorption band with some substructure between 195 and 225 nm. A second absorption band starts at wavelengths smaller than 180 nm. We refer to Weber [11], Gumanskaya *et al.* [12], and Meilman *et al.* [13] for the spectroscopic properties of Pr^{3+} doped $Y_3Al_5O_{12}$ crystals.

5d-4f luminescence usually originates from the bottom of the lowest 5d energy band to levels of the $4f^n$ configuration; the transition to the ground state being the most intense one.

Experimental Details

The fluoride crystals were grown by the hydrothermal synthesis technique by one of us (Khaidukov). They were not analysed for the concentration of the intentionally doped and unwanted impurities. The Ce^{3+} and Pr^{3+} concentrations reported in this work are the nominal concentrations determined from the amount of material weighted in prior to crystal growth. Single crystals with many facets and with dimensions of typically $4\times4\times4\,mm^3$ were obtained with this technique. The crystals were ground and polished to a thickness of about 2 mm with two plan-parallel faces. The Pr^{3+} doped $Y_3Al_5O_{12}$ crystal was grown in vacuum by horizontally oriented crystallization with the Bridgman technique. Pr^{3+} substitutes an Y^{3+} ion. Its concentration which amounts to about 0.8 mol%, was determined after growth by x-ray fluorescence. The crystal has dimensions of $\approx12\times20\times1.2\,mm^3$.

An ARC (Acton Research Corporation) vacuum monochromator with a Thorn EMI (type 9426) photomultiplier tube (PMT) was employed to study the scintillation properties of the crystals at wavelengths between 115 and 540 nm. For determining the emission spectra, the crystals under investigation were excited by means of continuous irradiation by x-rays from an x-ray tube with a copper anode operating at 35 kV. Each scintillation decay component including afterglow will then contribute to the recorded emission spectrum. The emission spectra presented in this work were corrected for the transmittance of the monochromator and the quantum efficiency of the PMT. Furthermore, a correction for the second order transmission of the monochromator was carried out. The absolute scale in the emission spectra in photons/(MeV·nm) was determined by comparison with the emission spectrum of a pure BaF_2 crystal recorded under identical experimental conditions. The estimated systematic error in the reported photon yields is about 10%.

For recording ^{137}Cs pulse height spectra, a crystal was coupled to the window of an XP2020Q photomultiplier tube with an optical coupling compound (Viscasil 60,000 cSt). The crystal was wrapped in teflon foil in order to obtain a good light collection on the photocathode. The energy resolution and the photoelectron yield were determined from the width and the position of the 662 keV photopeak in the pulse height spectrum. Scintillation decay time spectra were determined by single photon counting techniques. The decay spectra were corrected for dead time and counts caused by random coincidences. We refer to [14, 15] for more details on the experimental techniques described above.

Results and Discussion

$CsGd_2F_7$:Ce^{3+}: The host material $CsGd_2F_7$, which has a density of $5.5\,g/cm^3$, was doped with Ce^{3+} concentrations of 0.1, 0.3, 1, 3, and 10 mol%. The Ce concentration of the samples with nominal concentrations up to 1 mol% was verified by measuring the intensity of the Ce^{3+} 4f-5d optical absorption bands. The intensity ratio of the absorption bands belonging to different samples agrees with the ratio of the nominal Ce^{3+} concentrations in these samples. This still leaves the possibility for a systematic difference between the nominal and actual Ce concentrations in these samples. The same holds for the crystals with 3 and 10 mol% Ce. This will, however, not affect the conclusions drawn in this work.

Gd was used as a matrix forming element of the host crystal because it has a high atomic number resulting in a high density of the host crystal with a good stopping power for gamma rays. Furthermore, Gd^{3+} does not show absorption lines at wavelengths longer than 311 nm. It was anticipated that the bottom of the relaxed 5d band of Ce^{3+} in $CsGd_2F_7$ is located at a lower energy than the first excited state (^6P_J, J=7/2) of Gd^{3+}. Quenching of the Ce emission due to energy transfer from the excited Ce ions to this state is then energetically not possible. Instead, efficient Ce^{3+} luminescence may be expected due to an efficient energy transfer from the Gd sublattice to the Ce^{3+} ions.

The x-ray excited luminescence spectrum of a pure crystal shows a very weak (<10 photons/MeV) Gd^{3+} $^6P_{7/2}$-$^8S_{7/2}$ emission line at 311 nm. The emission spectrum of the crystal doped with 0.3 mol% Ce, see Figure 2, shows this same emission line along with a broad Ce 5d-4f emission band peaking at 340 nm. A quite similar luminescence spectrum was observed for a photon excited $RbGd_2F_7$:Ce crystal by Ellens *et al.* [16]. The Gd emission disappears and a small shift of the Ce emission band towards longer wavelengths is observed for Ce concentrations larger than 1 mol%. The wavelength integrated Ce emission intensity increases with the Ce concentration, see Figure 3, to a value of 6000 photons/MeV for the 10 mol% doped crystal. A study of the emission intensity of the crystal doped with 10 mol% Ce showed that thermal quenching of the luminescence starts to occur at temperatures beyond 400 K.

The decay time of the scintillation pulses created by

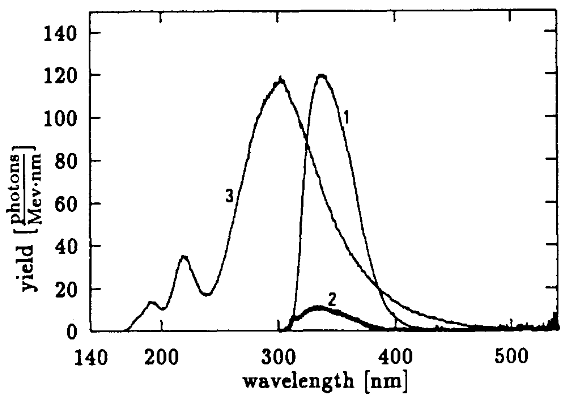

Figure 2: x-ray excited emission spectra of (1) $CsGd_2F_7$:10 mol% Ce^{3+}, (2) $CsGd_2F_7$:0.3 mol% Ce^{3+}, and (3) pure BaF_2.

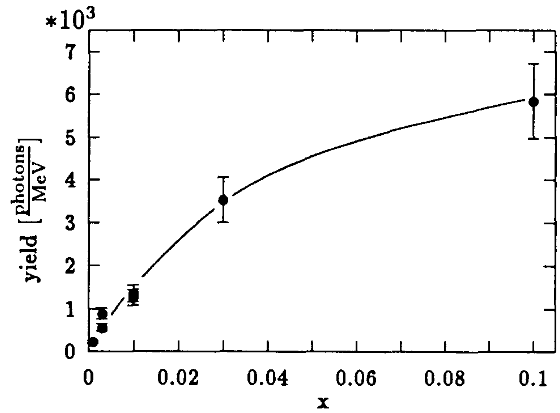

Figure 3: Integrated x-ray excited Ce^{3+} luminescence intensity of $CsGd_{2(1-x)}Ce_{2x}F_7$ crystals at room temperature.

662 keV γ-quanta in the crystals doped with 0.1, 0.3, and 1.0 mol% Ce were too long (>50 μs) to be measurable with our set-up. The scintillation decay spectra for the 3 and 10 mol% doped crystals are shown in Figure 4. The initial rise of the scintillation pulses in the first 2 ns of the spectra is caused by the time resolution of the set-up. The crystal doped with 3 mol% shows a slow Ce^{3+} scintillation component with a decay time of $\approx$25 μs which accounts for 98.5% of its total scintillation light output corresponding with 3450 photons/MeV. The rest, 1.5%, is caused by a fast Ce^{3+} scintillation component observable in the first 50 ns of the spectrum. For the 10 mol% doped crystal, the decay time of the slow component has decreased to about 3 μs. The intensity of the fast component has increased and accounts for 13% (780 photons/MeV) of the total Ce luminescence intensity. The decay of the fast component is non-exponential.

The pulse height spectrum of a ^{137}Cs source using the $CsGd_2F_7$:10 mol% Ce crystal is shown in Figure 5. A

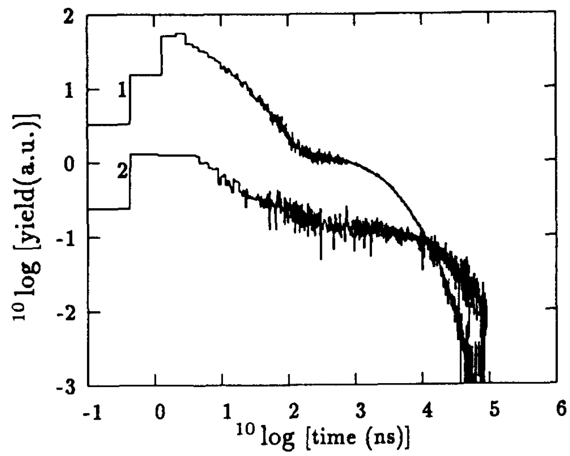

Figure 4: Scintillation decay spectra of (1) $CsGd_2F_7$:10 mol% Ce^{3+} and (2) $CsGd_2F_7$:3 mol% Ce^{3+}.

Canberra (model 1413) shaping amplifier with a shaping time of 8 μs was employed. The full width at half maximum of the 662 keV total absorption peak is 13.5%. From the position of the peak, we obtain a photo-electron yield of 900 photoelectrons/MeV.

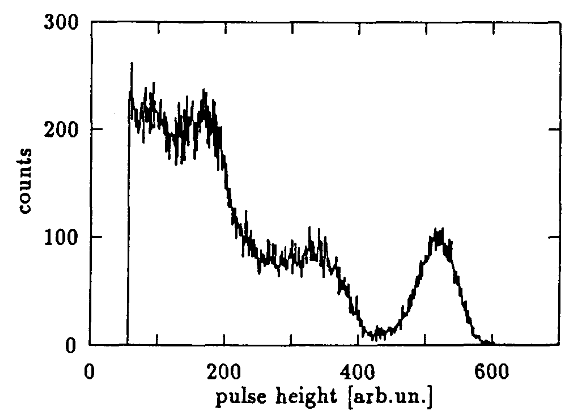

Figure 5: Pulse height spectrum of a ^{137}Cs source using a $\approx$4x4x2 mm^3 $CsGd_2F_7$:10 mol% Ce^{3+} crystal coupled to a Philips XP2020Q photomultiplier tube.

The observation of two distinct decay components suggests that there are at least two different mechanisms for the excitation of Ce^{3+} ions in $CsGd_2F_7$ crystals after an ionizing particle has been absorbed. Based on the 5d-4f luminescence properties of several other Ce^{3+} doped crystals [17], we expect a radiative decay time of 30-40 ns for the 5d excited state of Ce^{3+} in $CsGd_2F_7$ crystals. This value is of the same magnitude as the decay time of the observed fast scintillation component which indicates that one excitation mechanism must be very fast. We might think of instantaneous excitation of those Ce^{3+} ions which are present in the ionization track created by the absorbed ionizing particle. It is then expected that the number of instantaneous excitations is proportional to the number of Ce^{3+} ions in the track. This may explain why the fast component has only significant intensity for large Ce concentrations. The non-exponential decay character of the fast component may be attributed to quenching of the luminescence by energy transfer to Gd^{3+} or other quenching centers.

The presence of the slow component must be attributed to an energy transfer mechanism much slower than the radiative lifetime of the 5d level. We propose the following mechanism. After ionization, most of the excitations of the host lattice relax by phonon emission to the lowest excited state ($^6P_{7/2}$) of Gd^{3+}. The radiative lifetime of this state in other Gd based compounds like $LiGdF_4$ [18], $GdMgB_5O_{10}$ [19] is typically $\approx$10 ms. Within this lifetime, the excitation migrates over the Gd sublattice by transfer of the excitation energy via nearest neighbor Gd^{3+} ions; this is a well studied phenomenon in several Gd^{3+} based compounds [18, 19, 20]. Based on these studies, we envisage the following three transfer mechanisms:

i) $Gd^{3+} \xrightarrow{n\times} Gd^{3+} \rightarrow$ 4f-4f luminescence. The excitation migrates over the Gd sublattice until the $^6P_{7/2}$ level decays radiatively.

ii) $Gd^{3+} \xrightarrow{n\times} Gd^{3+} \rightarrow Q \rightarrow$ quenching. The migration terminates on a quenching center Q and disappears radiationless.

iii) $Gd^{3+} \xrightarrow{n\times} Gd^{3+} \rightarrow Ce^{3+} \rightarrow$ 5d-4f luminescence. The excitation energy migrates to a Ce^{3+} ion followed by 5d-4f luminescence.

Three decay rates for the $^6P_{7/2}$ level can now be introduced; the radiative decay rate $\Gamma_\nu \approx 100\,s^{-1}$, the transfer rate, Γ_q, to quenching centers, and the transfer rate $\Gamma_{Ce}(x)$ to the Ce ions which is assumed to depend on the Ce concentration x.

The intensity of the Gd 4f-4f emission is in this model given by $\Gamma_\nu/(\Gamma_\nu + \Gamma_q + \Gamma_{Ce})$. Since the observed 4f-4f emission intensity is very small for the pure crystal, we conclude that $\Gamma_q \gg \Gamma_\nu$. The light yield of the slow 5d-4f scintillation decay component is proportional to $\Gamma_{Ce}(x)/(\Gamma_\nu + \Gamma_q + \Gamma_{Ce}(x))$ and its decay time is proportional to $\approx \Gamma_{Ce}^{-1}$. The observed increase of the slow scintillation component and the decrease of its decay time with increasing x are both explained qualitatively if one assumes an increase of Γ_{Ce} with the Ce concentration. For small Ce concentrations, we expect that on the average, the number n of $Gd^{3+} \rightarrow Gd^{3+}$ transfer steps in the migration path to the Ce^{3+} will decrease with increasing concentration resulting in a larger transfer rate. However, at Ce concentrations of 3 and 10 mol% almost each Gd ion has a nearest neighbor Ce ion. The number of $Gd^{3+} \rightarrow Gd^{3+}$ transfer steps necessary to excite the Ce will then reduce to zero, and Γ_{Ce} is entirely determined by the $Gd^{3+} \rightarrow Ce^{3+}$ transfer rate. Similar to $LiGdF_4$:Ce [18], we expect that this transfer rate depends on the spectral overlap between the Gd^{3+} emission at 311 nm and the 4f-5d absorption band.

$CsGd_2F_7$:Pr^{3+}: The rare earth ion Pr^{3+} has two electrons in the 4f shell resulting in thirteen 4f energy levels. The highest excited 4f energy level ($^1S_0$) is located at an energy of about 47000 cm^{-1}, see Figure 1. Photon emissions or absorption caused by transitions between this excited state and the ground state are then expected at photon wavelengths of 213 nm. One may expect to observe 5d-4f luminescence if the bottom of the 5d band of Pr^{3+} ions doped in a suitable host lattice is located at a lower energy than the $^1S_0$ level. We have studied a crystal of $CsGd_2F_7$ doped with 2 mol% Pr^{3+}. Its optical absorption spectrum showed that the onset of the 4f-5d absorption band is located near 220 nm. So, in principle, the condition for 5d-4f luminescence is met. The x-ray excited luminescence spectrum did, however, not show 5d-4f emission bands. We only observed the Gd^{3+} emission line near 311 nm and sharp emission lines at wavelengths longer than 460 nm which are caused by 4f-4f transitions in Pr^{3+}. The absence of 5d-4f emissions is clearly related to the presence of Gd^{3+} in the host lattice. Excited electrons and holes in the host lattice will relax by phonon emission in the Gd^{3+} sublattice to the $^6P_{7/2}$ state of Gd^{3+}, which is located at a lower energy than the bottom of the lowest 5d band of Pr^{3+}.

K_2YF_5: Pr^{3+} : The host lattice K_2YF_5 has a density of 3.1 g/cm^3. The crystals, which were doped with 1 and 2 mol% Pr^{3+}, are slightly yellow coloured due to the presence of 4f-4f absorption lines in the Pr^{3+} ions. There are some cracks present in the crystals which may influence the accuracy of the reported photon yields/MeV.

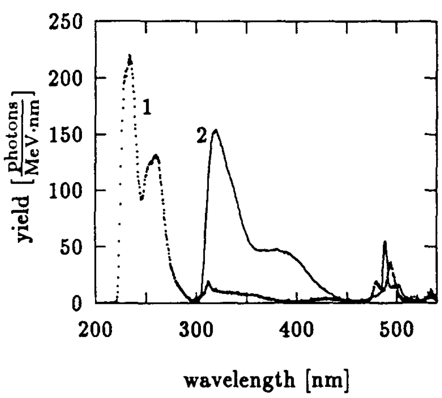

Figure 6: x-ray excited emission spectra of (1) K_2YF_5:2 mol% Pr^{3+} and (2) $Y_3Al_5O_{12}$:0.8 mol% Pr^{3+} at room temperature.

Figure 6 shows the x-ray excited emission spectrum of K_2YF_5 doped with 2 mol% Pr^{3+}. The two emission bands located at 230 and 260 nm are attributed to transitions from the bottom of the 5d band of Pr^{3+} to the ^3H_J and ^3F_J manifolds, see Figure 1. Evidently, the bottom of the 5d band is located at lower energy than the $^1S_0$ level. Transitions within the 4f shell of Pr^{3+} are responsible for the sharp emission lines between 470 nm and 510 nm. The presence of a trace impurity of Gd^{3+} is responsible for the weak emission line near 312 nm. The weak emission band between 300 nm and 380 nm is attributed to 5d-4f transitions in trace impurities of Ce^{3+}. Cross-luminescence, observable at vacuum ultra violet wavelengths in pure K_2YF_5 crystals [14], was not observed for the Pr^{3+}doped crystals. This is due to the presence of Pr^{3+} 4f-5d absorption bands at wavelengths shorter than 220 nm. The absolute light yield of the Pr^{3+} 5d-4f luminescence was found to be 3900 photons/MeV and 6900 photons/MeV for the crystal doped with 1 and 2 mol% Pr^{3+} respectively. The Pr^{3+} concentration at which the luminescence intensity is maximal has not yet been established.

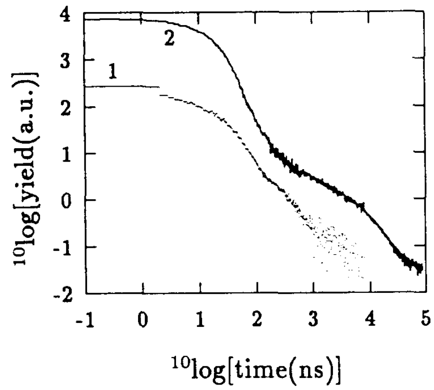

Figure 7: Scintillation decay spectra of (1) K_2YF_5:2 mol% Pr^{3+} and (2) $Y_3Al_5O_{12}$:0.8 mol% Pr^{3+} .

The decay time spectrum of the K_2YF_5 crystal doped with 2 mol% Pr^{3+} is shown in Figure 7. The spectrum reveals a fast decay component with a decay time of about 20 ns. This component is, however, rather weak, and accounts for only 5% (350 photons/MeV) of the total light yield. The dominating part (6550 photons/MeV) of the luminescence manifests itself as afterglow which lasts for several days after excitation of the crystal with x-rays. Intrinsic or extrinsic defects or impurities causing trapping of charge carriers resulting in a very slow energy transfer to the Pr^{3+} ions are probably responsible for the afterglow. Both the fast component and the afterglow could not be observed by an XP2020 photomultiplier tube. This tube has a glass window and is insensitive to photons with wavelengths smaller than 280 nm. This implies that the fast component and the afterglow are related to the 5d-4f luminescence bands of Pr^{3+}.

$Y_3Al_5O_{12}$:0.8 mol% Pr^{3+}: The room temperature x-ray excited luminescence spectrum of the crystal, which has a density of 4.55 g/cm^3, is shown in Figure 6. The Pr^{3+} 5d-4f emission bands are located between 300 and 460 nm which is at considerably longer wavelengths than observed for the Pr^{3+} doped K_2YF_5 crystals. The total integrated 5d-4f luminescence light yield amounts to 8000 photons/MeV. Weak emission lines due to transitions in the 4f shell of Pr^{3+} ions are located near 490 nm. Figure 8 shows the emission spectra recorded at 100 K and 425 K. The spectrum recorded at 100 K shows a new weak emission band between 240 and 280 nm. One can also distinguish, due to the narrowing of the 5d-4f emission bands, the transitions to the $^3H_4$ ground state at 316 nm and to the $^3H_5$ level at 336 nm. The integrated photon light yields over the wavelength intervals 240-280 nm, 300-460 nm, and 475-515 nm as a function of the temperature are shown in Figure 9. The dominating 5d-4f emission component located between 300 and 460 nm shows an almost constant intensity of 10700 photons/MeV between 150 and 250 K. Above 260 K, the emission starts to quench to a value of about 2000 photons/MeV near 425 K. Contrary to the 5d-4f luminescence, the intensity of the 4f-4f emission lines near 500 nm increases with increasing temperature. The weak emission band at 256 nm starts to develop when the temperature drops below 225 K and reaches an intensity of 150 photons/MeV at 100 K.

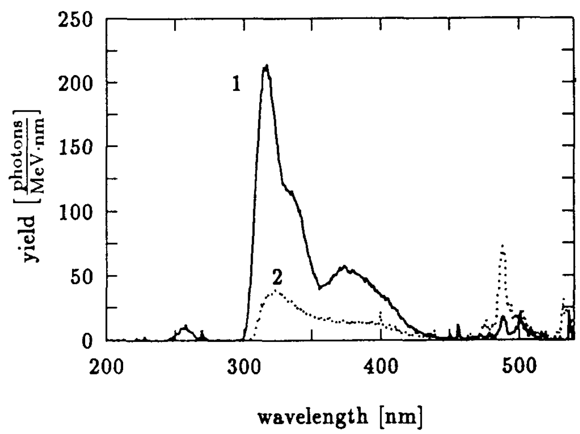

Figure 8: x-ray excited emission spectra of, solid curve (1), $Y_3Al_5O_{12}$:0.8 mol% Pr^{3+} at 100 K, and dotted curve (2) at 425 K.

The scintillation decay curve, see Figure 7, shows an intense exponential decay component with a decay time of 18 ns. This component accounts for more than 80% (6400 ph/MeV) of the total light yield. The other 20% (1600 ph/MeV) is rather slow and can be observed up to the 10 μs region.

Figure 10 shows the pulse height spectrum of a ^{137}Cs source obtained with the $Y_3Al_5O_{12}$:Pr^{3+} crystal, coupled to the window of an XP2020Q photomultiplier tube. A Canberra (model 1413) spectroscopy amplifier with a shaping time of 1 μs was employed. The photofraction is rather small, due to the absence of elements with a high atomic

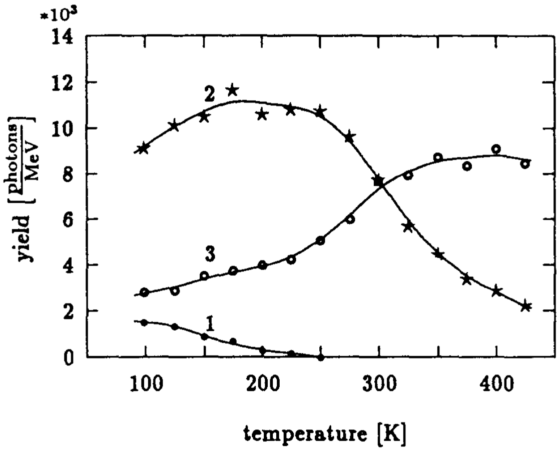

Figure 9: Integrated photon yields as a function of the temperature of the x-ray excited $Y_3Al_5O_{12}$:0.8 mol% Pr^{3+} crystal. 1) •, interval 240-280 nm multiplied by a factor of 10, 2) ⋆, 5d-4f luminescence in the interval 300-460 nm, 3) ∘, 4f-4f luminescence in the interval 475-515 nm multiplied by a factor of 10. The solid curves were drawn to guide the eye.

number in the host lattice. From the position of the 662 keV photopeak, a photoelectron (phe) yield of 1400±100 phe/MeV is obtained. A yield of 1650±150 phe/MeV was measured if a shaping time of 8 μs was employed. This yield is, considering reflection losses and the quantum efficiency of the photomultiplier tube, in accordance with the photon yield of 8000 photons/MeV.

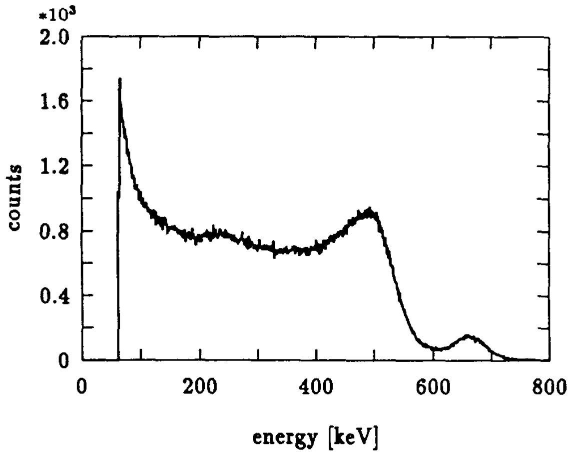

Figure 10: Pulse height spectrum of a ^{137}Cs source using the $Y_3Al_5O_{12}$:Pr^{3+} crystal coupled to a Philips XP2020Q photomultiplier tube.

The Pr^{3+} doped $Y_3Al_5O_{12}$ crystal shows an efficient and fast luminescence under x-ray and γ-ray excitation which implies that there is an efficient and fast energy transfer from the host lattice to the Pr^{3+} ions. Our results show a decay time of 18 ns for the main scintillation component. The same value was observed by Weber [11] for the decay of the photon excited 5d-4f luminescence. From this, we conclude that the excitation of Pr^{3+} ions is much faster than the decay time of the 5d excited state of Pr^{3+}. There are also similarities between the temperature quenching of x-ray excited Pr^{3+} 5d-4f luminescence, see Figure 9, and the photon excited luminescence. We refer to Weber [11] for an explanation of this quenching in terms of multiphonon relaxation of the d-electron to the 4f states of Pr^{3+}. The nonradiative decay of the 5d electron to 4f states may also explain qualitatively the observed increase of the 4f-4f luminescence intensity with increasing temperature, see Figure 9. We can think of two explanations for the origin of the new emission band at 256 nm; i) a 5d-4f transition originating from the bottom of the one but lowest 5d band of Pr^{3+} and terminating on the 4f ground state. The emission is quenched at temperatures above 200 K because of non-radiative relaxation to the lowest 5d band. ii) a broad intrinsic luminescence band of the host lattice. Only the part emitted between 240 and 280 nm is observed because the crystal is transparent in this wavelength interval.

Summary and Conclusions

In this work we have studied the scintillation properties of three host lattices doped with Ce^{3+} or Pr^{3+}. For the $CsGd_2F_7$ crystals, we observe with increasing Ce concentration the following trends: i) the photon yield/MeV increases, ii) the decay time of the slow Ce^{3+} scintillation decay component decreases, iii) the relative and absolute intensity of the fast Ce^{3+} scintillation component increases. A large photon yield/MeV, a fast decay time, and a large fast to slow ratio are highly desirable properties for a scintillator. For the $CsGd_2F_7$:Ce crystals each of these properties improve with increasing Ce concentration, and the crystal with 10 mol% is clearly the most interesting one. However, the decay time of the slow component is still too long and the intensity of the fast component is too low. Improvements are expected for Ce concentrations larger than 10 mol%.

The Pr^{3+} doped $CsGd_2F_7$ and K_2YF_5 crystals are very poor scintillation crystals because of the absence of fast scintillation components. Whether the properties of the Pr^{3+}doped K_2YF_5 crystals can be improved by increasing the Pr^{3+} concentration or by eliminating the trapping centers responsible for the intense afterglow has not been studied.

The $Y_3Al_5O_{12}$:Pr^{3+}crystal shows a scintillation light yield of 8000 photons/MeV; 80% is emitted as a fast component with a decay time of 18 ns and the rest is slow with a decay time of the order of 10 μs.

References

[1] D.F. Anderson, "Properties of the high density scintillator Cerium Flouride", *IEEE Trans. on Nucl. Sci.*, NS-36,

pp.137, 1989.

[2] W.W. Moses, S.E. Derenso, "Cerium fluoride, a new fast, heavy scintillator", *IEEE Trans. on Nucl. Sci.*, NS-36, pp.173, 1989.

[3] K. Takagi, T. Fukasawa, "Cerium activated Gd_2SiO_5 single crystal scintillator", *Appl. Phys. Lett.*, Vol.42(1), pp.43, 1983.

[4] C.L. Melcher, J.S. Schweitser, "A promising new scintillator: cerium-doped lutetium oxyorthosilicate", *Nucl. Instr. and Meth.*, Vol.A314, pp.212, 1992.

[5] R. Autrata, P. Schauer, Jiri Kvapil, Josef Kvapil, "A single crystal of $YAlO_3$:Ce^{3+} as a fast scintillator for SEM", *SCANNING*, Vol.5, pp.91, 1983.

[6] R. Autrata, P. Schauer, Jiri Kvapil, Josef Kvapil, "A single crystal of YAG - new fast scintillator in SEM", *J. Phys E: Sci. Instr.*, Vol.11, pp.707, 1978.

[7] P. Dorenbos, C.W.E. van Eijk, R.W. Hollander, P. Schotanus, "Scintillation properties of Nd^{3+} doped LaF_3 crystals", *IEEE Trans. Nucl. Sci.*, Vol.37(2), pp.119, 1990.

[8] J.L. Jansons, V.J. Krumins, Z.A. Rachko, J.A. Valbis, "Luminescence due to radiative transitions between valence band and upper core band in ionic crystals (crossluminescence)", *Phys. Stat. Sol. (b)*, vol.144, pp. 835, 1987.

[9] P. Dorenbos, R. Visser, C.W.E. van Eijk, J. Valbis, N.M. Khaidukov, "Photon yields and decay times of cross luminescence in ionic crystals", presented at the 1991 IEEE NS symposium, Santa Fe, USA, Nov. 5-9, 1991.

[10] K.A. Gschneidner, Jr. and L. Eyring, *Handbook on the Physics and Chemistry of Rare Earths*, Amsterdam: North-Holland Publishing Company, 1982, Vol.5, Chapter 46.

[11] M.J. Weber, "Nonradiative decay from 5d states of rare earths in crystals", *Solid State Communications.*, Vol.12, pp.741, 1973.

[12] E.G. Gumanskaya, M.V. Korshik, S.A. Smirnova, V.B. Pavlenko, A.A. Fedorov, "Interconfiguration luminescence of Pr^{3+} ions in $Y_3Al_5O_{12}$ and $YALO_3$ single crystals", *Opt. Spectrosc. (USSR)*, Vol.72, pp.86, 1992.

[13] M.L. Meilman, A.I. Kolomiitsev, A.M. Kevorkov, Kh.S. Bagdasarov, "Ultraviolet luminescence in interconfigurational electronic transitions in praseodymium-activated YAG crystals", *Opt. Spectrosc. (USSR)*, Vol. 57(2), pp.145, 1984.

[14] P. Dorenbos, R. Visser, C.W.E. van Eijk, J. Valbis, "Photon yields and decay times of cross-luminescence in ionic crystals", *IEEE Trans. NS*, Vol. 39(4), pp.506, 1992.

[15] P. Dorenbos, J.T.M. de Haas, R. Visser, C.W.E. van Eijk, R.W. Hollander, "Absolute light yield measurements on BaF_2 crystals and the quantum efficiency of several photomultiplier tubes", *IEEE Trans. NS*, this issue, 1993.

[16] A. Ellens, S.J. Kroes, J. Sytsma, G. Blasse, N.M. Khaidukov, "Luminescence of some ternary gadolinium fluoride crystals", *Materials Chem. and Phys.*, Vol.30, pp.127, 1991.

[17] Li-Ji Lyu, D.S. Hamilton, "Radiative and nonradiative relaxation measurements in Ce^{3+} doped crystals", *J. of Luminescence*, Vol.48 & 49, pp.251, 1991.

[18] H.S. Kiliaan, A. Meijerink, G. Blasse, "Energy transfer phenomena in Li(Y,Gd)F_4:Ce,Tb", *J. of Luminescence*, Vol.35, pp.155, 1986.

[19] G. Blasse, "Basic and applied research on phosphors based on gadolinium compounds", *Phys. Stat. Sol. (a)*, Vol.130, K85, 1992.

[20] G. Blasse, "Energy transfer phenomena in the system (Y,Ce,Gd,Tb)F_3", *Phys. Stat. Sol. (a)*, Vol.73, pp.205, 1982.